

# Symmetry Enforced Self-Learning Monte Carlo Method Applied to the Holstein Model

Chuang Chen,<sup>1,2</sup> Xiao Yan Xu,<sup>3,\*</sup> Junwei Liu,<sup>3</sup> George Batrouni,<sup>4,5,6,7</sup> Richard Scalettar,<sup>8</sup> and Zi Yang Meng<sup>1,9,†</sup>

<sup>1</sup>Beijing National Laboratory for Condensed Matter Physics and Institute of Physics,  
Chinese Academy of Sciences, Beijing 100190, China

<sup>2</sup>School of Physical Sciences, University of Chinese Academy of Sciences, Beijing 100190, China

<sup>3</sup>Department of Physics, Hong Kong University of Science and Technology, Clear Water Bay, Hong Kong, China

<sup>4</sup>Université Côte d'Azur, INPHYNI, CNRS, 0600 Nice, France

<sup>5</sup>Beijing Computational Science Research Center, Beijing, 100193, China

<sup>6</sup>MajuLab, CNRS-UNS-NUS-NTU International Joint Research Unit UMI 3654, Singapore

<sup>7</sup>Centre for Quantum Technologies, National University of Singapore, 2 Science Drive 3, 117542 Singapore

<sup>8</sup>Physics Department, University of California, Davis 95616 USA

<sup>9</sup>CAS Center of Excellence in Topological Quantum Computation and School of Physical Sciences,  
University of Chinese Academy of Sciences, Beijing 100190, China

(Dated: May 14, 2018)

Self-learning Monte Carlo method (SLMC), using a trained effective model to guide Monte Carlo sampling processes, is a powerful general-purpose numerical method recently introduced to speed up simulations in (quantum) many-body systems. In this work, we further improve the efficiency of SLMC by enforcing physical symmetries on the effective model. We demonstrate its effectiveness in the Holstein Hamiltonian, one of the most fundamental many-body descriptions of electron-phonon coupling. Simulations of the Holstein model are notoriously difficult due to the combination of the typical cubic scaling of fermionic Monte Carlo and the presence of extremely long autocorrelation times. Our method addresses both bottlenecks. This enables simulations on large lattices in the most difficult parameter regions, and evaluation of the critical point for the charge density wave transition at half-filling with high precision. We argue that our work opens a new research area of quantum Monte Carlo (QMC), providing a general procedure to deal with ergodicity in situations involving Hamiltonians with multiple, distinct low energy states.

*Introduction* — Electron-phonon coupling is ubiquitously present in condensed matter materials, responsible not only for the nature of basic, single-particle, properties such as the resistance and renormalized quasiparticle mass[1], but also for more exotic collective phenomena such as metal-insulator transitions[2], charge density wave (CDW) phases[3, 4], and superconductivity (SC)[5, 6]. Electron-phonon coupling also has a rich interplay with electron-electron interactions[7, 8]. The Holstein Hamiltonian [9], which describes spinful electrons hopping on a lattice and interacting locally with a phonon degree of freedom, is one of the most simple models of this rich physics, incorporating both polaron formation [10–14] in the dilute limit, and collective insulating CDW and SC transitions. Despite its simplicity, investigation of the Holstein Hamiltonian is extremely challenging, especially within an exact treatment of both its bosonic (phonon) and electronic degrees of freedom.

With the help of the Lang-Firsov transformation, QMC studies of Holstein (and related) models in 1D can be performed for large systems and interesting parameter regimes [15]. The case of retarded interaction in 1D is addressed with directed-loop QMC [16]. There have also been many attempts to explore the phase diagram of the 2D Holstein and Holstein-Hubbard models [17–34]. Recent studies of the metal to CDW phase transition in the weak-coupling regime [32] and the competition between CDW and superconductivity at intermediate coupling strength with phonon dispersion [34] and different Fermi

surface topologies [33] have broadened the understanding of the model and its relevance to the microscopic mechanism of superconductivity.

However, for 2D and 3D, these QMC methods are limited by the necessity of the expensive evaluation of a fermion determinant which enters the weight of the configuration, and also long autocorrelation times even away from critical points [35]. Thus, even though a sign problem[36, 37] is absent for the Holstein model, reliable results for the complete phase diagram, in particular for the most interesting intermediate-coupling strength of the model are still missing. The cost of treating fermion determinants is largely unavoidable. However, the ergodicity problem has been successfully solved, on an instance-by-instance basis, in a number of classical and QMC approaches [38–40]. It remains the key bottleneck of many others[41] (apart from the sign problem). Indeed, the failure of ergodicity challenges determinant and constrained path QMC [42, 43], lattice gauge theory simulations[44, 45], impurity solvers[46, 47] in dynamical mean field theory, and configuration interaction methods in quantum chemistry[48, 49].

A recently developed self-learning Monte Carlo (SLMC) method [50–54], based on a trained effective model to guide the Monte Carlo simulation [55, 56], shows substantial improvements over traditional Monte Carlo methods. The central idea of SLMC is to make use of learning algorithms to construct an approximate effective action which can be very rapidly calculated. An exact simulation is recovered by the evaluation of the full determinant which, however, can be done relatively infrequently, owing to the accuracy of the learned effective action. In 2D problems in which fermions coupled to bosonic fluctuations exhibit itinerant quantum critical points,  $L \times L$  spatial lattices with  $L$  up to 100 can be investigated at

\* wanderxu@gmail.com

† zymeng@iphy.ac.cn

high temperature [52] and  $L$  up to 48 has been achieved at low temperatures with  $\beta \sim L$  scaling [57, 58].

In this Letter, we show how SLMC can be applied to the Holstein Hamiltonian. Our key results are the following: (1) long autocorrelation times can be greatly reduced by designing an effective bosonic Hamiltonian for the phonon fields which incorporates a global  $Z_2$  symmetry in the original model; (2) computational complexity is reduced from roughly  $O(L^{11})$  to  $O(L^7)$ , i.e., a speedup of  $O(L^4)$  in SLMC over traditional MC method; (3) with such improvements, simulations of lattice sizes up to  $L = 20$  are possible, allowing the evaluation of the metal to CDW transition temperature to an order of magnitude higher accuracy than previously available. These advantages open a new research area of QMC for strongly correlated systems where SLMC provides powerful and general procedure to improve ergodicity.

*Model*—We study the Holstein Hamiltonian,

$$H = H_{\text{el}} + H_{\text{lat}} + H_{\text{int}}, \quad (1)$$

with

$$\begin{aligned} H_{\text{el}} &= -t \sum_{\langle ij \rangle \sigma} c_{i\sigma}^\dagger c_{j\sigma} - \mu \sum_{i\sigma} n_{i\sigma}, \\ H_{\text{lat}} &= \sum_i \left( \frac{M\Omega^2}{2} X_i^2 + \frac{1}{2M} P_i^2 \right), \\ H_{\text{int}} &= g \sum_{i\sigma} n_{i\sigma} X_i. \end{aligned} \quad (2)$$

$H_{\text{el}}$  describes spinful electrons hopping on a 2D square lattice of linear size  $L$ ,  $H_{\text{lat}}$  is the free phonon Hamiltonian, and  $H_{\text{int}}$  describes a local coupling between electron density and the phonon displacement at site  $i$ .  $\Omega$  is the phonon frequency, and  $g$  is the electron-phonon coupling. We set  $M = t = 1$  as the units of mass and energy, and focus on half-filling ( $\mu = \frac{g^2}{\Omega^2}$ ,  $\langle n_i \rangle = 1$ ). On a square lattice,  $W = 8t$  is the non-interacting bandwidth and  $\lambda = \frac{g^2}{M\Omega^2 W} = \frac{g^2}{8t\Omega^2}$  provides a dimensionless measure of the electron-phonon coupling. In this work, we focus on the intermediate coupling strength  $\lambda = 0.5$  ( $g = 1$ ,  $\Omega = 0.5$ ), a parameter regime which is more challenging than that explored in several recent works [32, 34].

One can see some of the fundamental physics of the Holstein model by considering the atomic limit ( $t = 0$ ). Completing the square in  $\frac{\Omega^2}{2} X_i^2 + g n_i X_i$ , and integrating out the phonon degrees of freedom, leads to an effective attraction  $\frac{g^2}{\Omega^2}$  between spin up and spin down electrons, and to pair formation [29]. At low temperatures, when  $t$  is made nonzero, these pairs can either organize into an insulating CDW pattern (which tends to happen at half-filling), or condense into a SC phase (at incommensurate density). On the other hand, integrating out the fermions leads to a potential energy surface for the phonons with two minima, at  $X_i = 0$  and  $X_i = -\frac{2g}{\Omega^2}$ , corresponding to empty ( $n_i = 0$ ) and double ( $n_i = 2$ ) occupation respectively. The large barrier at single occupation  $n_i = 1$  between these minima is the fundamental causes of long autocorrelation times in QMC simulations.

Several QMC methods have been used to simulate the Holstein model [10, 11, 13, 17, 18, 22, 32, 59–62]. Here we use

determinant quantum Monte Carlo (DQMC) [63–65], which is especially effective in dimension  $D > 1$  and in the large coupling regime. In this approach, the inverse temperature  $\beta = L_\tau \Delta\tau$  is discretized (we use  $\Delta\tau = 0.1$  in this work), and a path integral expression for the partition function is constructed in terms of the quantum coordinates in space  $i \in L^2$  and imaginary time index  $l = 1, 2, \dots, L_\tau$ . The fermions are integrated out, resulting in a weight  $\omega[X]$  for the phonon fields  $X_{i,l}$  which consists of a product of a bosonic piece  $e^{-S_{\text{Bose}} \Delta\tau}$  with  $S_{\text{Bose}} = \frac{\Omega^2}{2} \sum_{i,l} X_{i,l}^2 + \sum_{i,l} \left( \frac{X_{i,l+1} - X_{i,l}}{\Delta\tau} \right)^2$  and a fermion contribution  $(\det M(\{X_{i,l}\}))^2$ . The square comes from the fact that the two spin species couple to the phonon field in the same way, giving rise to identical determinants. Here  $M$  is a matrix of dimension  $N = L^2$ .

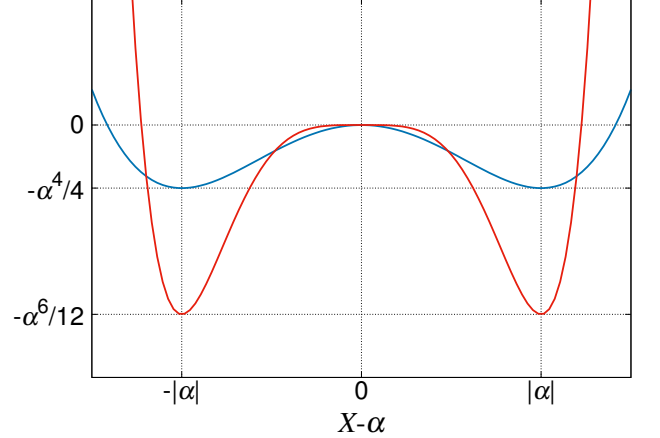


FIG. 1. The symmetric functions used to construct the phonon potential have minima at  $\pm|\alpha|$  with  $\alpha = -\frac{g}{\Omega^2}$ . The blue line is  $\frac{1}{4}(X - \alpha)^4 - \frac{\alpha^2}{2}(X - \alpha)^2$  and red line is  $\frac{1}{6}(X - \alpha)^6 - \frac{\alpha^2}{4}(X - \alpha)^4$ .

Local updates of a single phonon coordinate  $X_{i,l}$  can be done with a computation cost  $O(N^2)$ , so that a sweep through all  $N L_\tau$  components scales as  $N^3 L_\tau = L^6 L_\tau$  in  $D = 2$ . The first computational bottleneck, associated with the fermionic degrees of freedom is immediately evident: Doubling the linear lattice size  $L$  results in a 64-fold increase in computation time in  $D = 2$ . Part of the origin of the second bottleneck is also clear from the form of  $S_{\text{Bose}}$ . The phonon degrees of freedom on adjacent imaginary time slices  $l$  are tightly coupled, especially so as  $\Delta\tau$  becomes small. Moves of a single coordinate are thus energetically unfavorable. A block update of all the imaginary time phonon coordinates  $l$  of a single spatial lattice site  $i$  helps surmount this problem. It is also important to tune the value of the change in the block update  $\Delta X = \frac{2g}{\Omega^2}$ , to shift the phonon fields between the two minima. More details can be found in Sec. A of the Supplemental Materials (SM) [66].

However, even with the local and block updates, the autocorrelation time  $\tau_L$  of DQMC for the Holstein model is still found to increase rapidly with system size, as shown in Fig 2 (a). (Further aspects of Fig 2 will be discussed later.) We find  $\tau_L \sim L^{5.1}$ , much worse than the dynamic critical exponent  $\tau_L \sim L^z$  with  $z = 2$  associated with classical Monte Carlo

simulations with local update, e.g. of the Ising model near its critical point[38]. Such autocorrelation times lead to a situation where in 2D,  $L \sim 10 - 14$  is at the limit of DQMC simulations. It is important to note that large  $\tau_L$  occurs even away from any critical point, but in this work we focus on the most difficult situation – critical slowing down near  $T_c$ .

**SLMC** — To overcome these problems, we apply SLMC to the Holstein model. The first step[50–54], is to obtain an effective model by self-learning on configurations generated with DQMC updates according to Eq. 1. Here, at each temperature studied, we use 80,000 configurations obtained for  $L = 6$  systems to train the effective model  $H^{\text{eff}}$ , which we choose to have polynomial form,

$$H^{\text{eff}}[X] = E_0 + J_i X_i + J_{ij} X_i X_j + \dots \quad (3)$$

where  $E_0$  is the zeroth order background,  $J_i$  are the first order terms,  $J_{ij}$  are second order terms,  $\dots$ , and indices  $i$  and  $j$  are now combined space-imaginary time coordinates. Such a form is very natural, as after tracing out the fermions, the bosonic fields acquire long-range interactions in space-time beyond the bare level. One can make use of the symmetry of the original model to further reduce the number of parameters in the effective model, consequently reduce the effort and uncertainty in the fitting step.

The two potential minima of the Holstein model are symmetric with respect to  $X = -\frac{g}{\Omega^2} \equiv \alpha$ . We build this into the effective model by representing the potential by functions with these two minima (Fig. 1 and see Sec. C of the SM for details). We find that for the phonon fields in the Holstein model, two functions are sufficient to fit an appropriate barrier width and height. Our effective model thus has the following form (up to a constant),

$$\begin{aligned} -\beta H^{\text{eff}} = & J_k \sum_{i\tau} (X_{i\tau+1} - X_{i\tau})^2 \\ & + J_p \sum_{i\tau} \left( \frac{1}{4} (X_{i\tau} - \alpha)^4 - \frac{\alpha^2}{2} (X_{i\tau} - \alpha)^2 \right) \\ & + J'_p \sum_{i\tau} \left( \frac{1}{6} (X_{i\tau} - \alpha)^6 - \frac{\alpha^2}{4} (X_{i\tau} - \alpha)^4 \right) \\ & + J_{nn} \sum_{\langle ij \rangle \tau} (X_{i\tau} - \alpha)(X_{j\tau} - \alpha) \\ & + J'_{nn} \sum_{i \langle \tau \tau' \rangle} (X_{i\tau} - \alpha)(X_{i\tau'} - \alpha), \end{aligned} \quad (4)$$

where the  $J_k$ -term comes from the phonon kinetic energy,  $J_p$  and  $J'_p$ -terms are functions which produce the two global minima of Fig. 1 and  $J_{nn}$  and  $J'_{nn}$  are the nearest neighbor interaction in the spatial and temporal directions, respectively. Longer range interactions are found to contribute little to the weight and are thus omitted (we have tried spatial interaction to  $L/2$  and temporal interaction encompassing 10 time slices). One key remark here is this effective model captures a global  $Z_2$  symmetry, namely, a global mirror operation on  $X$  with axis  $\alpha$  leaving  $H^{\text{eff}}$  invariant.

With the effective model in the form of Eq. 4, the training procedure is straightforward. Given a configuration  $X$  of the

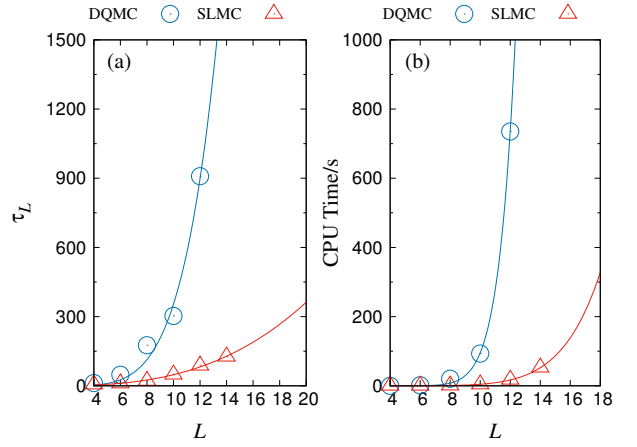


FIG. 2. (a) Comparison of autocorrelation time of the CDW structure factor versus  $L$  for DQMC and SLMC. Simulations were done at the critical point  $T_c$  for the CDW transition. SLMC greatly suppresses the autocorrelation time, with dynamical exponent  $z \sim 2.9$ , while for DQMC,  $z \sim 5.1$ . (b) Comparison of CPU time to obtain one statistically independent configuration ( $\tau_L$  sweeps) between DQMC and SLMC. Power-law fitting gives  $\sim L^{11}$  for DQMC and  $\sim L^7$  for SLMC. Including the prefactor, SLMC provides a  $\times 50$  speedup for  $L = 12$  and  $\times 300$  speedup for  $L = 20$ .

phonon field and its corresponding weight  $\omega[X]$ , generated in DQMC, we have

$$-\beta H^{\text{eff}}[X] = \ln(\omega[X]). \quad (5)$$

Combining Eq. (4) and Eq. (5), optimized values of  $J_k$ ,  $J_p$ ,  $J'_p$ ,  $J_{nn}$  and  $J'_{nn}$  (shown in Tab. S1 in the SM) can be readily obtained through a multi-linear regression [50–52] using all the configurations prepared with DQMC. Note for each temperature, we only train  $H^{\text{eff}}$  from small system size ( $L = 6$ ), but use it to larger systems (up to  $L = 20$ ) in SLMC.

We use the effective model to guide the Monte Carlo simulation of the original model, namely, propose many updates of the phonon fields according to Eq. 4, this is the so-called cumulative update in SLMC [51, 52]. We then calculate the acceptance ratio of the final phonon field configuration via the expensive fermion determinant only rarely. There are two advantages of SLMC over DQMC. First, the effective model is purely bosonic and its local update is  $O(1)$  since it bypasses the calculation of fermion determinants. Second, since the effective model is bosonic, global updates, such as Wolff and other cluster update schemes [38, 39], are easy to implement. This is crucial since cluster updates in conventional DQMC actually worsen the scaling from  $O(N^3 L_\tau)$  to  $O(N^4 L_\tau)$ .

The Holstein model exhibits a finite temperature metal to CDW insulator phase transition at half-filling belonging to the 2D Ising universality class [32, 34]. As discussed in detail in Sec. D of the SM, we designed a modified Wolff cluster update on the effective model, by building the cluster in space and including all sites of temporal columns which addresses additional long autocorrelation times associated with proximity to the critical point. This modified Wolff update successfully reduces the autocorrelation time of Monte Carlo

simulations from  $L^{5.1}$  to  $L^{2.9}$  (as shown in Fig. 2(a)). So the dynamical exponent is reduced by  $\Delta z \geq 2$ , an equivalent improvement to that provided by cluster moves in the classical Ising model [38, 39].

Using this combination of updates on the effective model, we propose cumulative move [51, 52] of the phonon field for the original model, combined with a final acceptance ratio,

$$A(X \rightarrow X') = \min \left\{ 1, \frac{\exp(-\beta H[X']) \exp(-\beta H^{\text{eff}}[X])}{\exp(-\beta H[X]) \exp(-\beta H^{\text{eff}}[X'])} \right\}, \quad (6)$$

which ensures detailed balance and hence simulation of the original Holstein  $H[X]$ .

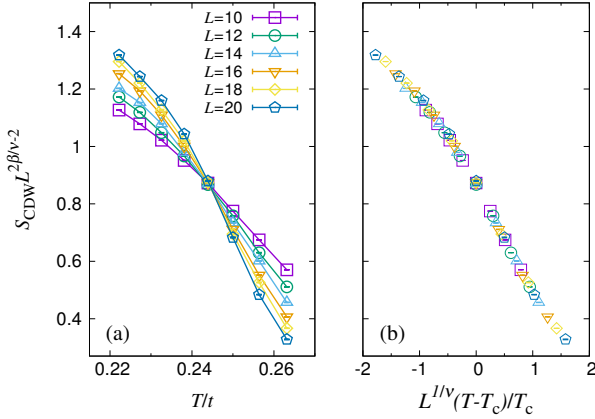


FIG. 3. (a) Finite size scaling analysis showing  $S_{\text{CDW}} L^{-7/4}$  versus  $T/t$ . The critical point  $T_c = 0.244(3)$  is determined from the crossing of finite size data. (b) Data collapse of  $S_{\text{CDW}} L^{-7/4}$  versus  $L^{1/\nu} (T - T_c)/T_c$  with  $\nu = 1$ . Note the quality of the collapse is better than that in Ref. [34], due to larger  $L$  obtained with SLMC.

**Results** — To compare SLMC and DQMC, Fig. 2 (a) depicts the autocorrelation time of the CDW structure factor  $S_{\text{CDW}} = \frac{1}{L^2} \sum_{ij} (-1)^{i+j} (\langle n_i n_j \rangle - \langle n_i \rangle \langle n_j \rangle)$  for DQMC and SLMC. We have chosen the most challenging criterion, both by analyzing a long range quantity associated with the order parameter (which has much longer correlations than simple local quantities like the energy) and also by tuning the temperature to  $T = T_c$ . To compare in an equal footing, a MC step in DQMC is defined as a sweep with local update plus 4 block updates; whereas a MC step in SLMC is defined as local plus Wolff-cluster updates. As can be seen from the fitting of the  $\tau_L \sim L^z$ , severe critical slowing down is observed in DQMC, with dynamical exponent ( $z \sim 5.1$ ); on the other hand,  $z \sim 2.9$  in SLMC. A reduction of  $\Delta z \geq 2$  is achieved – equivalent to the improvement of cluster over local moves in classical Ising model [38, 39].

In Fig. 2(b), we show how much CPU time is needed to obtain a statistically independent phonon configuration. SLMC provides a  $\times 50$  speedup for  $L = 12$ , and more than  $\times 300$  speedup for  $L = 20$ . With this dramatic improvement, we are able to simulate the Holstein model in the difficult parameter regime ( $\lambda \sim 0.5$ ) and determine the critical point with high precision. At the critical point, the finite size scaling behavior

$S_{\text{CDW}}/L^2 = L^{-2\beta/\nu} f\left(L^{1/\nu} \left(\frac{T-T_c}{T_c}\right)\right)$  is expected, where  $\beta = \frac{1}{8}$ ,  $\nu = 1$  are the 2D Ising critical exponents. Fig. 3(a) shows  $L^{-7/4} S_{\text{CDW}}$  versus  $T$  for  $L = 10$  to 20. Their crossing point yields the critical temperature  $T_c = 0.244(3)$ . In Fig. 3(b), we further rescale the horizontal-axis with  $L \left(\frac{T-T_c}{T_c}\right)$  giving an excellent data collapse. Our value of  $T_c$  represents a substantial improvement over existing work which typically reports maximal lattice sizes of  $L = 10 \sim 12$  [34].

**Conclusions** — In this Letter, we applied SLMC to simulations of the electron-phonon interaction in the Holstein model, where QMC is very difficult due to long autocorrelation times and the expense of the fermion determinant evaluation. By imposing a global  $Z_2$  symmetry in the effective model of SLMC, we have successfully captured the global minima of the phonon potential. In addition, we designed a Wolff-cluster update in the effective model which greatly reduces the autocorrelation time challenge which has hampered simulation of the Holstein model for several decades.

With these improvements on the effective model, SLMC simulation of the Holstein Hamiltonian can be pushed to larger system sizes, comparable with other interacting fermion systems [67–70] or itinerant quantum criticality models [57, 58, 71]). This allows for much more reliable determination of critical properties.

The idea of imposing symmetry in the effective model can be generalized to other situations. For example, in the Hubbard and Hubbard-like models, one can introduce a continuous auxiliary field  $\phi$  to decouple the interaction in the spin channel,  $\alpha \phi (n_\uparrow - n_\downarrow)$ . High barriers interfere with movement between minima at  $n_\uparrow - n_\downarrow = \pm 1$ . Block updates in DQMC can be used [72] but are very time consuming, especially as the lattice size increases. Our work suggests that SLMC can improve this situation by proposing global updates based on effective models like Eq. (4) with appropriate symmetry to capture the minima and lead to a big reduction in autocorrelation time. Construction of large scale moves is not only computationally much inexpensive within the context of effective models like Eq. (4), but it is also much easier to incorporate intuitive physical pictures of the low energy configurations. This suggests SLMC will provide a general framework for improving ergodicity beyond the Holstein model illustrated here.

If successful, outstanding problems such as spectral properties in the Mott insulator, or the recently discovered phenomena of symmetric mass generation [73, 74] could be explored more efficiently. Potential applications extend outside condensed matter physics to, for example, QMC simulations of shell model Monte Carlo [75] in high-energy physics. The key requirement for our application of SLMC is only that the interactions can be decoupled to continuous bosonic fields associated with fermion bilinears, where several minima are present.

**Acknowledgments** — C.C. and Z.Y.M. acknowledge the valuable discussions with Martin Hohenadler and Fakher Asaad on the Holstein model, and thank the support from the Ministry of Science and Technology of China under Grant No. 2016YFA0300502, the key research program of the Chinese Academy of Sciences under Grant No. XDPB0803, the

National Natural Science Foundation of China under Grants No. 11421092, 11574359 and 11674370, and the National Thousand-Young Talents Program of China. X.Y.X. acknowledges the support of HKRGC through grant C6026-16W and also gratefully acknowledges the hospitality of Institute of Physics, Chinese Academy of Sciences. We thank the following institutions for allocation of CPU time: the Center for

Quantum Simulation Sciences in the Institute of Physics, Chinese Academy of Sciences; the Tianhe-1 platform in the National Supercomputer Center in Tianjin. GGB acknowledges support from the Université Côte d'Azur IDEX Jedi. The work of RTS is supported by the U.S. Department of Energy under grant de-sc0014671.

- 
- [1] F. Giustino, *Rev. Mod. Phys.* **89**, 015003 (2017).
  - [2] J. E. Han, E. Koch, and O. Gunnarsson, *Phys. Rev. Lett.* **84**, 1276 (2000).
  - [3] G. Grüner and A. Zettl, *Physics Reports* **119**, 119 (1985).
  - [4] G. Grüner, *Rev. Mod. Phys.* **60**, 1129 (1988).
  - [5] K. Bennemann and J. Ketterson, *The Physics of Conventional and Unconventional Superconductors* (Springer-Verlag Berlin Heidelberg, 2001).
  - [6] J. Bardeen, L. N. Cooper, and J. R. Schrieffer, *Phys. Rev.* **106**, 162 (1957).
  - [7] M. L. Kulić and R. Zeyher, *Phys. Rev. B* **49**, 4395 (1994).
  - [8] F. Gebhard, *The Mott Metal-Insulator Transition* (Springer-Verlag Berlin Heidelberg, 1997).
  - [9] T. Holstein, *Annals of Physics* **8**, 325 (1959).
  - [10] P. E. Kornilovitch, *Phys. Rev. Lett.* **81**, 5382 (1998).
  - [11] M. Hohenadler, H. G. Evertz, and W. von der Linden, *Phys. Rev. B* **69**, 024301 (2004).
  - [12] L.-C. Ku, S. A. Trugman, and J. Bonča, *Phys. Rev. B* **65**, 174306 (2002).
  - [13] A. Macridin, G. A. Sawatzky, and M. Jarrell, *Phys. Rev. B* **69**, 245111 (2004).
  - [14] J. Bonča, S. A. Trugman, and I. Batistić, *Phys. Rev. B* **60**, 1633 (1999).
  - [15] M. Hohenadler and W. von der Linden, “Lang-firsov approaches to polaron physics: From variational methods to unbiased quantum monte carlo simulations,” in *Polarons in Advanced Materials*, edited by A. S. Alexandrov (Springer Netherlands, Dordrecht, 2007) pp. 463–502.
  - [16] M. Weber, F. F. Assaad, and M. Hohenadler, *Phys. Rev. Lett.* **119**, 097401 (2017).
  - [17] R. T. Scalettar, N. E. Bickers, and D. J. Scalapino, *Phys. Rev. B* **40**, 197 (1989).
  - [18] F. Marsiglio, *Phys. Rev. B* **42**, 2416 (1990).
  - [19] G. Levine and W. P. Su, *Phys. Rev. B* **42**, 4143 (1990).
  - [20] R. M. Noack, D. J. Scalapino, and R. T. Scalettar, *Phys. Rev. Lett.* **66**, 778 (1991).
  - [21] G. Levine and W. P. Su, *Phys. Rev. B* **43**, 10413 (1991).
  - [22] M. Vekić, R. M. Noack, and S. R. White, *Phys. Rev. B* **46**, 271 (1992).
  - [23] M. Vekić and S. R. White, *Phys. Rev. B* **48**, 7643 (1993).
  - [24] P. Niyaz, J. E. Gubernatis, R. T. Scalettar, and C. Y. Fong, *Phys. Rev. B* **48**, 16011 (1993).
  - [25] E. Berger, P. Valášek, and W. von der Linden, *Phys. Rev. B* **52**, 4806 (1995).
  - [26] H. Zheng and S. Y. Zhu, *Phys. Rev. B* **55**, 3803 (1997).
  - [27] E. A. Nowadnick, S. Johnston, B. Moritz, R. T. Scalettar, and T. P. Devereaux, *Phys. Rev. Lett.* **109**, 246404 (2012).
  - [28] E. A. Nowadnick, S. Johnston, B. Moritz, and T. P. Devereaux, *Phys. Rev. B* **91**, 165127 (2015).
  - [29] S. Johnston, E. A. Nowadnick, Y. F. Kung, B. Moritz, R. T. Scalettar, and T. P. Devereaux, *Phys. Rev. B* **87**, 235133 (2013).
  - [30] Y. Murakami, P. Werner, N. Tsuji, and H. Aoki, *Phys. Rev. B* **88**, 125126 (2013).
  - [31] T. Ohgoe and M. Imada, *Phys. Rev. Lett.* **119**, 197001 (2017).
  - [32] M. Weber and M. Hohenadler, *ArXiv e-prints* (2017), arXiv:1709.01096 [cond-mat.str-el].
  - [33] I. Esterlis, B. Nosarzewski, E. W. Huang, B. Moritz, T. P. Devereaux, D. J. Scalapino, and S. A. Kivelson, *ArXiv e-prints* (2017), arXiv:1711.01493 [cond-mat.str-el].
  - [34] N. C. Costa, T. Blommel, W.-T. Chiu, G. Batrouni, and R. T. Scalettar, *Phys. Rev. Lett.* **120**, 187003 (2018).
  - [35] M. Hohenadler and T. C. Lang, “Autocorrelations in quantum monte carlo simulations of electron-phonon models,” in *Computational Many-Particle Physics*, edited by H. Fehske, R. Schneider, and A. Weisse (Springer-Verlag Berlin Heidelberg, 2008) pp. 357–366.
  - [36] E. Y. Loh, J. E. Gubernatis, R. T. Scalettar, S. R. White, D. J. Scalapino, and R. L. Sugar, *Phys. Rev. B* **41**, 9301 (1990).
  - [37] M. Troyer and U.-J. Wiese, *Phys. Rev. Lett.* **94**, 170201 (2005).
  - [38] R. H. Swendsen and J.-S. Wang, *Phys. Rev. Lett.* **58**, 86 (1987).
  - [39] U. Wolff, *Phys. Rev. Lett.* **62**, 361 (1989).
  - [40] O. F. Syljuåsen and A. W. Sandvik, *Phys. Rev. E* **66**, 046701 (2002).
  - [41] D. Ceperley, *AIP Conference Proceedings* **690**, 85 (2003).
  - [42] F. Assaad and H. Evertz, *Lecture Notes in Physics*, Vol. 739 (2008).
  - [43] S. Zhang, eprint arXiv:cond-mat/9909090 (1999), cond-mat/9909090.
  - [44] G. Burgio, M. Fuhrmann, W. Kerler, and M. Müller-Preussker, *Phys. Rev. D* **75**, 014504 (2007).
  - [45] A. Amato, G. Bali, and L. B., arXiv:1512.00806 [hep-lat] (2015).
  - [46] P. Sémon, G. Sordi, and A.-M. S. Tremblay, *Phys. Rev. B* **89**, 165113 (2014).
  - [47] P. Seth, I. Krivenko, M. Ferrero, and O. Parcollet, *Comp. Phys. Comm.* **200**, 274 (2016).
  - [48] J. Shepherd, G. Booth, and A. Alavi, *The Journal of Chemical Physics* **136**, 244101 (2012).
  - [49] R. Thomas, C. Overy, G. Booth, and A. Alavi, *J. Chem. Theory Comput.* **10**, 1915 (2014).
  - [50] J. Liu, Y. Qi, Z. Y. Meng, and L. Fu, *Phys. Rev. B* **95**, 041101 (2017).
  - [51] J. Liu, H. Shen, Y. Qi, Z. Y. Meng, and L. Fu, *Phys. Rev. B* **95**, 241104 (2017).
  - [52] X. Y. Xu, Y. Qi, J. Liu, L. Fu, and Z. Y. Meng, *Phys. Rev. B* **96**, 041119 (2017).
  - [53] Y. Nagai, H. Shen, Y. Qi, J. Liu, and L. Fu, *Phys. Rev. B* **96**, 161102 (2017).
  - [54] H. Shen, J. Liu, and L. Fu, *ArXiv e-prints* (2018), arXiv:1801.01127 [cond-mat.str-el].
  - [55] L. Huang and L. Wang, *Phys. Rev. B* **95**, 035105 (2017).
  - [56] L. Huang, Y.-f. Yang, and L. Wang, *Phys. Rev. E* **95**, 031301 (2017).
  - [57] Z. H. Liu, X. Y. Xu, Y. Qi, K. Sun, and Z. Y. Meng, *ArXiv*

- e-prints (2017), arXiv:1706.10004 [cond-mat.str-el].
- [58] Z. H. Liu, X. Y. Xu, Y. Qi, K. Sun, and Z. Y. Meng, ArXiv e-prints (2018), arXiv:1801.00127 [cond-mat.str-el].
  - [59] P. E. Spencer, J. H. Samson, P. E. Kornilovitch, and A. S. Alexandrov, Phys. Rev. B **71**, 184310 (2005).
  - [60] M. Berciu, A. S. Mishchenko, and N. Nagaosa, EPL (Europhysics Letters) **89**, 37007 (2010).
  - [61] R. H. McKenzie, C. J. Hamer, and D. W. Murray, Phys. Rev. B **53**, 9676 (1996).
  - [62] R. M. Noack and D. J. Scalapino, Phys. Rev. B **47**, 305 (1993).
  - [63] R. Blankenbecler, D. J. Scalapino, and R. L. Sugar, Phys. Rev. D **24**, 2278 (1981).
  - [64] J. E. Hirsch, Phys. Rev. B **31**, 4403 (1985).
  - [65] F. Assaad and H. Evertz, in *Computational Many-Particle Physics*, Lecture Notes in Physics, Vol. 739, edited by H. Fehske, R. Schneider, and A. Weiße (Springer Berlin Heidelberg, 2008) pp. 277–356.
  - [66] See Supplemental Material for details on the implementation of the DQMC and SLMC algorithms of Holstein model..
  - [67] C. N. Varney, C.-R. Lee, Z. J. Bai, S. Chiesa, M. Jarrell, and R. T. Scalettar, Phys. Rev. B **80**, 075116 (2009).
  - [68] Z. Y. Meng, T. C. Lang, S. Wessel, F. F. Assaad, and A. Muramatsu, Nature **464**, 847 (2010).
  - [69] F. Parisen Toldin, M. Hohenadler, F. F. Assaad, and I. F. Herbut, Phys. Rev. B **91**, 165108 (2015).
  - [70] Y. Q. Qin, Y.-Y. He, Y.-Z. You, Z.-Y. Lu, A. Sen, A. W. Sandvik, C. Xu, and Z. Y. Meng, Phys. Rev. X **7**, 031052 (2017).
  - [71] X. Y. Xu, K. Sun, Y. Schattner, E. Berg, and Z. Y. Meng, Phys. Rev. X **7**, 031058 (2017).
  - [72] R. T. Scalettar, R. M. Noack, and R. R. P. Singh, Phys. Rev. B **44**, 10502 (1991).
  - [73] Y.-Y. He, H.-Q. Wu, Y.-Z. You, C. Xu, Z. Y. Meng, and Z.-Y. Lu, Phys. Rev. B **94**, 241111 (2016).
  - [74] Y.-Z. You, Y.-C. He, A. Vishwanath, and C. Xu, ArXiv e-prints (2017), arXiv:1711.00863 [cond-mat.str-el].
  - [75] S. Koonin, D. Dean, and K. Langanke, Physics Reports **278**, 2 (1997).
  - [76] M. Hasenbusch and S. Meyer, Physics Letters B **241**, 238 (1990).



# Supplemental Material: Symmetry Enforced Self-Learning Monte Carlo Method Applied to the Holstein Model

## Appendix A: DQMC for the Holstein model

As discussed in the main text, the Holstein model describes electrons hopping on a lattice and interacting with local phonon modes. Before introducing the implementation of SLMC on the Holstein model, we first give a short review of the DQMC algorithm, based mainly on Ref. [29].

We define  $K \equiv H_{\text{el}} + H_{\text{lat}}$  as the non-interacting terms for the electron and lattice (phonon) degrees of freedom. To implement DQMC, we start with partition function

$$Z = \text{Tr}(e^{-\beta H}) = \text{Tr}(e^{-\Delta\tau H_{\text{int}}} e^{-\Delta\tau K})^L + O((\Delta\tau)^2). \quad (\text{S1})$$

The Trotter-Suzuki decomposition is performed by discretizing  $\beta$  into  $L_\tau$  segments with  $\Delta\tau = \frac{\beta}{L_\tau}$ .

By tracing out the fermions, the partition function is expressed as an integral over the phonon fields,

$$Z = \int dX e^{-S_{\text{Bose}}\Delta\tau} \det M_\uparrow \det M_\downarrow, \quad (\text{S2})$$

where  $M_\sigma = I + B_L^\sigma B_{L-1}^\sigma \cdots B_1^\sigma$  with  $B_l^{\uparrow(\downarrow)} = e^{-\Delta\tau g X(l)} e^{-\Delta\tau K}$ ,  $S_{\text{Bose}} = \frac{\Omega^2}{2} \sum_{i,l} X_{i,l}^2 + \sum_{i,l} \left( \frac{X_{i,l+1} - X_{i,l}}{\Delta\tau} \right)^2$ .

The key quantity in DQMC is the single-particle Green function

$$[G^\sigma(l)]_{ij} = [I + B_l^\sigma \cdots B_1^\sigma B_L^\sigma \cdots B_{l+1}^\sigma]_{ij}^{-1}, \quad (\text{S3})$$

which is used to evaluate the acceptance ratio and to obtain physical observables. The ratio of fermion determinants

$$R = R^\uparrow R^\downarrow = \frac{\det M'^\uparrow \det M'^\downarrow}{\det M^\uparrow \det M^\downarrow}, \quad (\text{S4})$$

is used to accept or reject updates to the phonon field. If the update is local, a fast  $O(1)$  evaluation of  $R$  is possible:

$$R^\sigma = 1 + (1 - [G^\sigma(l)]_{ii} [\Delta^\sigma(i, l)]_{ii}). \quad (\text{S5})$$

However, the change in the phonon field alters the Green function. For local updates an  $O(N^2)$  procedure is provided by the Sherman-Morrison formula (compared to an  $O(N^3)$  scaling of a direct recalculation of  $G$ ). Since only one  $B$  matrix is changed from  $B^\sigma(l)$  to  $B'^\sigma(l) = [I + \Delta^\sigma(i, l)] B^\sigma(l)$ , where  $\Delta^\sigma(i, l)$  only has one non-zero element,  $[\Delta^\sigma(i, l)]_{jk} = \delta_{ik} \delta_{jk} [\exp(-g\Delta\tau \Delta X_{i,l}) - 1]$ , and

$$[G^\sigma(l)]' = G^\sigma(l) - \frac{G^\sigma(l) \Delta^\sigma(i, l) [I - G^\sigma(l)]}{1 + [1 - G_{ii}^\sigma(l)] \Delta_{ii}^\sigma(i, l)}. \quad (\text{S6})$$

As discussed in the main text, to overcome the barrier of two minima in the phonon potential, a block update is applied. By changing the phonon coordinate for all time slices of one site uniformly through a reflection with respect to the average phonon displacement ( $X(i, \tau) \rightarrow -X(i, \tau) - 2g/\Omega^2$ ).

## Appendix B: SLMC for the Holstein model

SLMC [50–52, 54], based on a trained effective model to guide Monte Carlo simulation, is proposed as a general method to simulate (quantum) many-body systems. As described in Ref [50–52] and in the main text, SLMC is comprised of four steps. In the case of Holstein model discussed in the work. We first generate 80,000 configurations of small size  $L = 6$  from DQMC. Second, at each temperature ( $\beta$  from 3.8 to 4.5, with  $\Delta\tau = 0.1$  and only considering 10 time slices in the training) we train an effective model by using data from the first step. Third, we simulate the effective model with many local and global moves, i.e., cumulative updates. Finally, the proposed updates of the effective model are accepted/rejected by applying detailed balance, described in Eq. 6, of the original model. In general, as shown here, as long as the effective model is a good description of the original Hamiltonian, the speedup of SLMC over conventional MC methods can be substantial. This leads us to the next section on how to design a good effective model.

## Appendix C: Designing the effective model

A good effective model is essential for SLMC. As described in Appendix A, after tracing out the fermion degrees of freedom in DQMC, one obtains an expression for the partition function involving only an integration over the phonon fields degree of freedom. However, to evaluate the determinant which enters the resulting weight for the phonons is numerically very slow. This is the reason we need a simpler, bosonic effective model to accelerate this step. We consider the atomic limit, where the phonon fields can be isolated on single sites, then the phonon field potential has the form  $\frac{\Omega^2}{2} X_i^2 + g n_i X_i - \mu n_i$ . As discussed in the main text, when  $g \neq 0$ , it is easy to see there are two potential minima at  $X_i = 0$  and  $X_i = -\frac{2g}{\Omega^2}$ , with electron filling  $n_i = 0$  and  $n_i = 2$ , respectively. Note that there is also a maximum in the middle  $X_i = -\frac{g}{\Omega^2} \equiv \alpha$ . Integrating the function  $X_i(X_i - 2\alpha)(X_i - \alpha)^a$  with odd  $a$  will give exactly the shape of two minima and one maximum in the phonon potential. This is how we obtained the functional forms  $\frac{1}{4}(X_{i\tau} - \alpha)^4 - \frac{\alpha^2}{2}(X_{i\tau} - \alpha)^2$  and  $\frac{1}{6}(X_{i\tau} - \alpha)^6 - \frac{\alpha^2}{4}(X_{i\tau} - \alpha)^4$  in the  $J_p$  and  $J'_p$  terms in the effective model in Eq. 4 in the main text.

By also considering the momentum term for phonons, the spatial and temporal interaction terms among the phonons, the

effective Hamiltonian with  $a = 1, 3$  terms takes the form

$$\begin{aligned}
-\beta H^{\text{eff}} = & J_k \sum_{i\tau} (X_{i\tau+1} - X_{i\tau})^2 \\
& + J_p \sum_{i\tau} \left( \frac{1}{4} (X_{i\tau} - \alpha)^4 - \frac{\alpha^2}{2} (X_{i\tau} - \alpha)^2 \right) \\
& + J'_p \sum_{i\tau} \left( \frac{1}{6} (X_{i\tau} - \alpha)^6 - \frac{\alpha^2}{4} (X_{i\tau} - \alpha)^4 \right) \\
& + J_{nn} \sum_{\langle ij \rangle \tau} (X_{i\tau} - \alpha)(X_{j\tau} - \alpha) \\
& + J'_{nn} \sum_{i \langle \tau \tau' \rangle} (X_{i\tau} - \alpha)(X_{i\tau'} - \alpha). \quad (\text{S1})
\end{aligned}$$

With Eq. S1 for the effective model, and configurations generated from DQMC, we perform multi-linear regression and obtain values of  $J_k$ ,  $J_p$ ,  $J'_p$ ,  $J_{nn}$  and  $J'_{nn}$ . As an example, Table S1 lists the values for  $L = 6$ ,  $\beta = \beta_c = 4.1$ ,  $\lambda = 0.5$ .

TABLE S1. Optimized values of  $J_k$ ,  $J_p$ ,  $J'_p$ ,  $J_{nn}$  and  $J'_{nn}$  obtained through a multi-linear regression [50–52] using all the configurations prepared with DQMC on parameters  $L = 6$ ,  $\beta = 4.1$ ,  $\lambda = 0.5$ .

$J_k$	$J_p$	$J'_p$	$J_{nn}$	$J'_{nn}$
5.00E1	1.39E-2	-3.05E-4	7.17E-3	7.67E-2

The effective model at other temperatures, is obtained in the similar manner.

#### Appendix D: Wolff update of the effective Hamiltonian

In this last section, we discuss how to build the modified Wolff-cluster update of the effective model. In the Wolff-

cluster update for the 2D or 3D Ising model, the probability of adding a spin to the cluster is  $P_{\text{add}} = 1 - e^{-2|J|\beta}$ , where  $2|J|$  is the energy cost when breaking a bond. For the effective model of the Holstein Hamiltonian, the phonon fields are continuous. The Wolff update for the effective model is therefore similar to that in the XY model [76], where the probability of adding a field to the cluster is

$$P_{\text{add}} = 1 - \exp[-2\beta(\hat{n} \cdot s_i)(\hat{n} \cdot s_j)]. \quad (\text{S1})$$

In the Holstein model, for the phonon fields, the probability of adding a field to the cluster is

$$P_{\text{add}} = 1 - \exp \left( 2\Delta\tau \sum_{\tau} J_{nn}(X_{i\tau} - \alpha)(X_{j\tau} - \alpha) \right). \quad (\text{S2})$$

Since there are very strong interactions along the temporal direction ( $J_k$  is more than  $10^3$  times larger than  $J_{nn}$ ), we will only use the  $J_{nn}$  term to build clusters in spatial planes and include sites in the entire temporal column in the cluster, hence the sum over  $\tau$  in Eq. S2. We then reflect all phonon fields in the cluster with respect to the symmetry axis  $X = \alpha$ . As the effective model has a global  $Z_2$  symmetry about the same axis, the acceptance ratio of the cluster update is one. In addition to the Wolff-cluster update, we also sweep over the space-time lattice of the phonon fields with local updates. The combination defines the global move proposal of the phonon field for the original model.